

Robust Pose Invariant Face Recognition using Coupled Latent Space Discriminant Analysis

Abhishek Sharma, Murad Al Haj, Jonghyun Choi, Larry S. Davis,
and David W. Jacobs

*Institute for Advanced Computer Studies
University of Maryland, College Park
College Park, MD 20742*

Abstract

We propose a novel pose-invariant face recognition approach which we call Discriminant Multiple Coupled Latent Subspace framework. It finds sets of projection directions for different poses such that the projected images of the same subject are maximally correlated in the latent space. Discriminant analysis with artificially simulated pose errors in the latent space makes it robust to small pose errors caused due to a subject's incorrect pose estimation. We do a comparative analysis of three popular learning approaches: Partial Least Squares (PLS), Bilinear Model (BLM) and Canonical Correlational Analysis (CCA) in the proposed coupled latent subspace framework. We also show that using more than two poses simultaneously with CCA results in better performance. We report state-of-the-art results for pose-invariant face recognition on CMU PIE and FERET and comparable results on MultiPIE when using only 4 fiducial points and intensity features.

Keywords: pose-invariant-face recognition, coupled latent space, PLS, CCA, discriminant coupled subspaces.

1. Introduction

Face recognition is a very challenging problem. Research in this area spans a wide range of statistical and geometric pattern recognition algorithms for tackling difficulties such as pose, illumination and expression variation. Most successful face recognition approaches require accurate alignment and feature correspondence between the face images to be compared. In many real-life scenarios face images appear in different poses causing correspondence problem. There has been a large body of work dealing with pose variation, but still fast and accurate recognition is a challenge. For a comprehensive and recent survey of pose invariant face-recognition see. [3] [1].

We can regard a face image as a vector in \mathfrak{R}^D . The coordinate axes defined for each pixel will constitute a *representation scheme* (\mathcal{S}) for the face

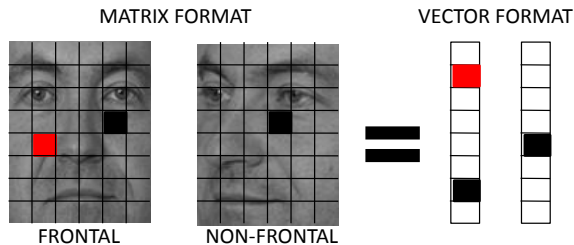


Figure 1: An example showing lack of correspondence due to missing regions and region displacement for pose variation. Black and red blocks indicate region displacement and missing region, respectively.

which is basically the set of column vectors of an identity matrix in \mathbb{R}^D space. Corresponding pixels across different subjects' faces roughly correspond to the same facial region in the absence of pose difference. This *feature correspondence* facilitates comparison. In fact, feature correspondence is essential for comparison based on a learned model. For faces especially, it has been shown to be crucial [4]. Unfortunately, face images under different poses lose feature correspondence because of missing facial regions, unequal dimensions and/or *region displacements*. Region displacement refers to the same facial region at different indices in feature vectors (see Fig.1).

We propose to obtain pose-specific representation schemes \mathcal{S}_i 's so that the projection of face vectors onto the appropriate representation scheme will lead to correspondence in the common projected space, which facilitates direct comparison. A representation scheme can also be regarded as a collection of projection directions, which we refer to as a *projector*. Intuitively, projectors are feature extractors through which the common information from multiple poses is collected and transferred to a common representation scheme which we term as *latent space*. Given a set of projectors \mathcal{S}_p and \mathcal{S}_q for gallery pose p and probe pose q . \mathcal{S}_p and \mathcal{S}_q can be used to project the gallery and probe images in the latent space where direct comparison can be done due to feature correspondence. The pose-specific projectors and associated latent space taken together are termed as *Correspondence Latent Subspace* or CLS because projection into the latent space provides correspondence.

In a preliminary version of the paper, we showed the conditions under which such latent spaces exist and used Partial Least Square (PLS) [19, 20, 18] to obtain them. Our work shows that linear projection to latent space is an effective solution for pose-invariant face recognition, which is considered to be a highly non-linear problem [12, 38, 22, 40]. Surprisingly, our approach with simple intensity features outperformed previously published work and we report state-of-the-art results on CMU PIE data for pose invariant face recognition.

Based on this general model, the pose-invariant face recognition problem reduces to estimation of the the gallery and probe pose and obtaining an appropriate CLS for recognition. We require a training set of face images in gallery and probe poses to learn CLS for these poses. In this work, we assume prior

knowledge of *ground-truth* gallery and probe poses. Ground-truth pose refers to the pose which is reported in the dataset. We also require training data with face images roughly in gallery and probe poses. The subject identities in training data and testing data are different and mutually exclusive. These assumptions are quite standard for learning based methods and have been used by many researchers in the past [14, 15, 38, 22, 12, 33, 39, 2, 40, 13, 9].

Our simple PLS based framework worked well for CMU PIE dataset, which has face images in tightly controlled acquisition scenario that ensures that the ground-truth poses are very close to the actual poses. But the same framework did not perform as expected on less controlled and larger datasets e.g. FERET [16] and MultiPIE [29]. On one hand, larger gallery size requires more discriminative features for classification but our previous approach is generative and does not use label information to learn projectors that are discriminative. On the other hand, a less controlled acquisition scenario gives rise to *pose errors*, which refers to the situation where the actual pose of the face image differs from the projector learned for that pose. Although the difference is small (generally around $\pm 10^\circ$), it can cause loss of correspondence which affects the performance. It can occur due to wrong pose estimation or head movement at the time of acquisition. Presence of pose errors is supported from significant difference between the estimated poses [5] and the ground-truth poses [6] for FERET dataset and our own experiments to estimate pose (subsection IV.E).

In order to make our framework practically applicable we need to account for large gallery sizes and pose errors. So, we extend our original work to a two-stage framework for pose invariant face recognition. The first stage learns pose-specific representation schemes for gallery/probe pose pairs (which we assume to be known beforehand) using a training set that has face images in roughly the same poses. The second stage learns discriminative directions in the Correspondence Latent Subspace (CLS) with three added advantages:

- Providing an identity based discriminative representation which is known to outperform generative representation [10].
- Achieving insensitivity to pose errors that are present in real-life as well as controlled scenarios.
- Exploiting multiple face samples per person in different poses for supervised learning, which was otherwise not possible due to modality difference.

We empirically noticed the improvement due to all these factors in the overall performance and report state-of-the-art pose recognition results for 2D based methods on CMU PIE and FERET and comparable to best published results on MultiPIE. A theoretical and empirical comparison between three popular methods CCA, PLS and BLM for learning CLS is done under different scenarios. We have also made the hand-annotated fiducial points for FERET and MultiPIE publicly available to promote research with these datasets.

This is an extended version of our conference paper [11]. The original conference version does not include the second stage discriminative learning and the results on FERET and MultiPIE. However, the conference version had a more detailed explanation of PLS which we omit here due to space constraints.

The rest of the paper is organized as follows: Section 2 gives a brief review of related approaches for pose invariant face recognition, Section 3 discusses some background. Section 4 describes the proposed approach followed by experimental analysis in section 5. Finally, we conclude and discuss salient points of the approach in section 6.

2. Previous Work

In [5], authors proposed a 3D Morphable Model for faces and use the fact that 3D face information extracted as *shape and texture* features remains the same across all poses. Hence, given a 2D image they constructed the corresponding 3D model and did matching in the 3D shape and texture space. This method performed well but is slow and requires 6-8 fiducial points. Moreover, the model heavily depends on the accurate extraction of 3D information from the 2D image which itself is a difficult problem. Recently Generic Elastic Models (GEMs) [34], showed that 3D depth information is not discriminative for pose invariant face recognition. Thus, a generic face depth map can be elastically deformed for a given 2D face to generate the corresponding 3D model leading to a fast version of 3DMM (2-3 seconds per image). They also extracted all the required 79 fiducial landmarks automatically. A different 3D geometric approach is based on stereo matching [31, 32] which uses four fiducial points to obtain the epipolar geometry and dynamic programming to match corresponding pixels. This approach has shown impressive performance on CMU PIE data set.

Locally Linear Regression or LLR [12] uses face images/patches to be the bases of the representation scheme, assuming that a face image/patch in pose p can be faithfully represented as a linear combination of a set of face images/patches and that the coefficients of linear combinations remain roughly constant across different poses. The coefficients of combination were learned using linear regression. Recently, [38] has reported significantly improved performance by using Ridge regression to estimate coefficients of a linear combination of a subject's face image in terms of training subject's images in the same pose and comparing the coefficients using normalized correlation. They have used Gabor features [37] at 5 hand-clicked facial points rather than simple pixel intensity to further enhance the performance. Similarly, the associate-predict model [40] divides face image in patches and extracts LBP [35], SIFT [36], Gabor [37] and Learning based descriptors LE [45] as features. Then each patch is associated with a similar patch from a training face image under approximately the same pose. This process is called association. In the prediction step, the associated patch's corresponding patch under gallery pose is used as a proxy for the original patch for matching purposes. All the above-mentioned approaches are essentially 2D approximations of the 3DMM theory which is not always correct. The strength of the approximation relies heavily on the validity of the

key assumption that the coefficients across pose remain almost equal. We argue that it may not hold for 2D face images unless it is forced explicitly [11, 9]. In [13], the authors realized this shortcoming and used Canonical Correlational Analysis (CCA) [18] to learn a pair of subspaces which make the projected images in the latent space maximally correlated. They also used a region based discriminative power map for face pixels modeled as a probability distribution [22]. We also use CCA to learn CLS but we use more than two poses simultaneously and pool information from multiple poses using latent space discriminant analysis. In [39], an attempt was made to learn the patch correspondence between frontal and non-frontal poses by using a batch version of Lucas-Kanade optical flow algorithm [41]. However, they use only two poses at a time and the discrimination is not based on label information.

TFA [14] and PLDA [15] use generative models to generate face images of a person across different poses from a common latent variable which they call Latent Identity Variable or LIV. At the time of recognition the images are transformed to the LIV space using a pose-specific linear transformation and recognition is carried out in that space. The accuracy of the approach depends on the validity of the factor model in terms of modeling the problem and the quality of the learned model parameters. They use the EM algorithm [42] to learn the model parameters which is prone to local minima and computationally intensive. Moreover, the assumption that a single LIV can be used to faithfully generate all the different poses of a person seems to be over simplified and may not be true. It becomes evident from poor performance even for small poses angles with simple intensity features. To improve the performance, they used 14 hand clicked points on face images to extract Gabor filter response which are more discriminative than raw pixels. But accurate location of fiducial-points in non-frontal images is still an open problem. A related patch-whole approach was proposed in [2] which tries to model the differential distribution of a gallery image patch and whole probe face. The advantage of this approach lies in the fact that due to patch-whole matching it is comparatively robust to small pose-estimation errors.

3. Background

In this section we discuss the details of Bilinear Model (BLM), Canonical Correlational Analysis (CCA) and Partial Least Square (PLS). All of these methods find a set of representation schemes which make the projected images of the same person *similar* to each other in the latent space. The definition of similar varies with the method, for instance CCA makes them maximally correlated while PLS maximizes the covariance between them. We also draw a theoretical comparison between these approaches.

Throughout this paper, superscripts denote indexing across identity, subscript denotes modality/pose, vectors are denoted as straight bold small alphabets (\mathbf{x}), variable/constants as small italic alphabets (a) and matrices as capital italic letters (A). Hence, the face image of i^{th} person in pose p is denoted as \mathbf{x}_p^i and a matrix of face samples in pose p as X_p .

3.1. Bilinear Model

Tannenbaum and Freeman [14] proposed a bilinear model for separating *style* and *content*. In pose invariant face recognition, style corresponds to pose and content corresponds to subject identity. They suggest methods for learning BLMs and using them in a variety of tasks, such as identifying the style of a new image with unfamiliar content, or generating novel images based on separate examples of the style and content. However, their approach also suggests that their content-style models can be used to obtain style invariant content representation that can be used for classification of a sample in a different style. Following their asymmetric model, they concatenate the i^{th} subject's images under M different modalities/poses ($\mathbf{y}_m^i : m = 1, 2, \dots, M$) to make a long vector \mathbf{y}^i and construct matrix Y having columns as \mathbf{y}^i with $i = \{1, 2, \dots, N = \#subjects\}$ such that:

$$Y = \begin{pmatrix} \mathbf{y}_1^1 & \mathbf{y}_1^2 & \dots & \mathbf{y}_1^N \\ \mathbf{y}_2^1 & \mathbf{y}_2^2 & \dots & \mathbf{y}_2^N \\ \vdots & \vdots & \ddots & \vdots \\ \mathbf{y}_M^1 & \mathbf{y}_M^2 & \dots & \mathbf{y}_M^N \end{pmatrix} \quad (1)$$

$$= (\mathbf{y}^1 \quad \mathbf{y}^2 \quad \dots \quad \mathbf{y}^N)$$

Modality matrices A_m which can be thought of as different representation schemes for a CLS model can be obtained by decomposing the matrix Y using SVD as -

$$Y = USV^T = (US)V^T = (A)B \quad (2)$$

A can be partitioned $A^T = (A_1^T \quad A_2^T \quad \dots \quad A_M^T)$ to give different CLS representation schemes A_m 's where m represents different poses.

3.2. CCA

CCA is a technique that learns a set of M different projectors from a set of observed *content* under M different *styles*. The projections of different *styles* of a particular *content* are maximally correlated in the projected space. Hence, CCA can be used to learn a common intermediate subspace in which projections of different pose images of the same subject will be highly correlated and recognition can be done on the basis of the correlation score. Given a set of face images of N different subjects under M different poses, CCA learns a set of K dimensional subspaces $W_m = \{\mathbf{w}_m^k : \mathbf{w}_m^k \in \mathfrak{R}^{D_m}; k = 1, 2, \dots, K\}$ for

$m = 1, 2, \dots, M$ such that [18] -

$$\begin{aligned}
& \begin{pmatrix} C_{11} & C_{12} & \dots & C_{1M} \\ C_{21} & C_{22} & \dots & C_{2M} \\ \vdots & \vdots & \ddots & \vdots \\ C_{M1} & C_{M2} & \dots & C_{MM} \end{pmatrix} \begin{pmatrix} \mathbf{w}_1^k \\ \mathbf{w}_2^k \\ \vdots \\ \mathbf{w}_M^k \end{pmatrix} \\
&= (1 + \lambda^k) \begin{pmatrix} C_{11} & 0 & \dots & 0 \\ 0 & C_{22} & \dots & 0 \\ \vdots & \vdots & \ddots & \vdots \\ 0 & 0 & \dots & C_{MM} \end{pmatrix} \begin{pmatrix} \mathbf{w}_1^k \\ \mathbf{w}_2^k \\ \vdots \\ \mathbf{w}_M^k \end{pmatrix} \quad (3) \\
&\Rightarrow CW = W(I + \Lambda)
\end{aligned}$$

Dm is the feature dimension of m^{th} style, $C_{ij} = \frac{1}{N} Y_i(Y_j)^T$ and Λ is the diagonal matrix of eigen-values λ^k , N is the number of training subjects and Y_i is defined in the previous sub-section. Eqn(3) is a generalized eigenvalue problem which can be solved using any standard eigensolver. The columns of the projector matrices W_m will span a linear subspace in modality m . So, when modalities are different poses we get a set of vectors spanning a linear subspace in each pose.

3.3. Partial Least Square

Partial Least Square analysis [23, 19, 20] is a regression model that differs from Ordinary Least Square regression by first projecting the regressors (input) and responses (output) onto a low dimensional latent linear subspace. The PLS projectors try to maximize the covariance between latent scores of regressors and responses. Hence, we can use PLS to obtain CLS for two different poses in the same way as BLM and CCA.

There are several variants of PLS analysis based on the factor model assumption and the iterative algorithm used to learn the latent space [19, 20]. Some of these variants facilitate the intuition behind PLS while some are faster but the objective function for all of them is the same. In this paper, we use the original NIPALS algorithm [19] to develop intuitions and a variant of NIPALS given in [20] to learn the projectors.

Following the same conventions as for BLM and CCA, Y_p represents a matrix containing face images in pose p as its columns. PLS greedily finds vectors \mathbf{w}_p and \mathbf{w}_q such that -

$$\begin{aligned}
& \max_{\mathbf{w}_p, \mathbf{w}_q} (\text{cov}[Y_p^T \mathbf{w}_p, Y_q^T \mathbf{w}_q]^2) \\
& s.t. \quad \|\mathbf{w}_p\| = \|\mathbf{w}_q\| = 1
\end{aligned} \quad (4)$$

3.4. Difference between BLM, PLS and CCA

Although BLM, CCA and PLS are trying to achieve the same goad but their end results are different due the difference in their objective functions. BLM

tries to preserve the variance present in different feature spaces and does not explicitly tries to make projected samples similar. It is interesting to compare the objective function of PLS with that of CCA to emphasize the difference between the two. CCA tries to maximize the correlation between the latent scores

$$\begin{aligned} & \max_{\mathbf{w}_p, \mathbf{w}_q} (\text{corr}[Y_p^T \mathbf{w}_p, Y_q^T \mathbf{w}_q]^2) \\ & \text{s.t. } \|\mathbf{w}_p\| = \|\mathbf{w}_q\| = 1 \end{aligned} \quad (5)$$

where,

$$\text{corr}(\mathbf{a}, \mathbf{b}) = \frac{\text{cov}(\mathbf{a}, \mathbf{b})}{\text{var}(\mathbf{a})\text{var}(\mathbf{b})} \quad (6)$$

putting the expression from (6) into (4) we get the PLS objective function as:

$$\begin{aligned} & \max_{\mathbf{w}_p, \mathbf{c}_q} ([\text{var}(Y_p^T \mathbf{w}_p)][\text{corr}(Y_p^T \mathbf{w}_p, Y_q^T \mathbf{w}_q)]^2[\text{var}(Y_q^T \mathbf{w}_q)]) \\ & \text{s.t. } \|\mathbf{w}_p\| = \|\mathbf{w}_q\| = 1 \end{aligned} \quad (7)$$

It is clear from (7) that PLS tries to correlate the latent score of regressor and response as well as captures the variations present in the regressor and response space too. CCA only tries to correlates the latent score hence CCA may fail to generalize well to unseen testing points and even fails to differentiate between training samples in the latent space under some restrictive conditions. A toy condition where PLS will succeed and both BLM and CCA will fail to obtain meaningful directions can be stated as follows - Suppose we have two sets of 3D points X and Y and x_i^j and y_i^j denote the j^{th} element of the i^{th} data point in X and Y . Suppose that the first coordinates of x_i and y_i are pair-wise equal and the variance of the first coordinate is very small and insufficient for differentiating different samples. The second coordinates are correlated with a correlation-coefficient $\rho \leq 1$ and the variance present in the second coordinate is ψ . The third coordinate is almost uncorrelated and the variance is $\gg \psi$.

$$\begin{aligned} \forall i, x_i^1 = y_i^1 = k & \Rightarrow \text{var}(X^1) = \text{var}(Y^1) = \alpha \ll \psi \\ \text{corr}(X^2, Y^2) = \rho & \text{ and } \text{var}(X^2), \text{var}(Y^2) \approx \psi \\ \text{corr}(X^3, Y^3) \approx 0 & \text{ and } \text{var}(X^3), \text{var}(Y^3) \gg \psi \end{aligned} \quad (8)$$

Under this situation CCA will give the first coordinate as the principal direction which projects all the data points in sets X and Y to a common single point in the latent space, rendering recognition impossible. BLM will find a direction which is parallel to the third coordinate, which preserves the inter-set variance but loses all the correspondence. PLS however, will opt for the second coordinate, which preserves variance (discrimination) as well as maintains correspondence which is crucial for our task of multi-modal recognition.

One major disadvantage of PLS as compared to CCA and BLM is the fact that extension of PLS to more than two modalities leads to poor set of projectors and also its very slow to learn them. So we cannot use PLS for our Discriminant

Multiple CLS framework (discussed later) where it is required to learn projectors for multiple poses together. On the other hand, CCA and BLM easily extend to multiple poses Eqn1 and Eqn3. However, the objective function and empirical results in [11] suggest that CCA is better than BLM for cross-modal recognition. Hence, we will be using CCA for the purpose of learning multiple CLS.

3.5. Linear Discriminant Analysis

There are two kinds of variation found in data samples - within-class and between-class variation. Within-class variation refers to variation present among the samples of the same class and between-class variation refers to the variation between the samples from different classes. Ideally, for a classification task we would like that the within-class variation is minimized and between-class variation is maximized simultaneously. The quantitative measure of within-class and between-class variation are the within-class scatter matrix S_W and between-class scatter matrix S_B -

$$S_W = \sum_{i=1}^C \sum_{j=1}^{N_c} (\mathbf{x}_i^j - \mathbf{m}_i)(\mathbf{x}_i^j - \mathbf{m}_i)^T$$

$$S_B = \sum_{i=1}^C (\mathbf{m}_i - \mathbf{m})(\mathbf{m}_i - \mathbf{m})^T$$
(9)

Linear discriminant analysis or LDA tries to find a projection matrix W that maximizes the ratio of S_B and S_W -

$$W_{opt} = \max_W \frac{|W^T S_B W|}{|W^T S_W W|}$$
(10)

It leads to the following generalized eigen-value problem -

$$S_B \mathbf{w}_i = \lambda_i S_W \mathbf{w}_i \quad i = \{1, 2, \dots, C - 1\}$$
(11)

Here, \mathbf{x}_i^j is the j^{th} sample for the i^{th} class, \mathbf{m}_i is the i^{th} class mean, \mathbf{m} is the total mean, C is the number of classes, N_c is the number of samples for class c , λ_i 's are the generalized eigen-values and $W = [\mathbf{w}_1 \quad \mathbf{w}_2 \quad \dots \quad \mathbf{w}_{C-1}]$.

4. Proposed Approach

In this section we first discuss the conditions under which CLS can account for pose difference and explain the PLS based framework for pose invariant face recognition and compare it to previously published works on the CMU PIE dataset. Then we evaluate the performance of the PLS based framework on larger and less controlled datasets e.g. FERET and MultiPIE to show that it does not perform as expected. Next, we carry out a performance drop study to understand the reason of poor performance and based on the observations we propose a novel extension of our original framework to account for the factors causing performance drop.

4.1. When CLS can account for pose

We can use a CLS framework to find linear projections that map images taken from two poses into a common subspace. However, a CLS based framework cannot be expected to lead to effective recognition when such projections do not exist. In this section, we show some conditions in which projections of images from two poses exist in which the projected images are perfectly correlated (and in fact equal). Then we show that these conditions hold for some interesting examples of pose-invariant face recognition. We should note that the existence of such projections is not sufficient to guarantee good recognition performance. We will empirically assess the actual performance of the proposed approach in section 6. In a number of cases, images taken in two poses can be viewed as different, linear transformations of a single ideal object. Let \mathbf{i} and \mathbf{j} denote column vectors containing the pixels of face images of the same person in two poses. We denote by r a matrix (or column vector) that contains an idealized version of \mathbf{i} and \mathbf{j} , such that we can write:

$$\mathbf{i} = A\mathbf{r} \quad \text{and} \quad \mathbf{j} = B\mathbf{r} \quad (12)$$

for some matrices A and B . We would like to know when it will be possible to find projection directions \mathbf{p}_1 and \mathbf{p}_2 which project sets of images into a 1D space in which these images are coupled. We consider a simpler case, looking at when the projections can be made equal. That is, when we can find \mathbf{p}_1 and \mathbf{p}_2 such that for any \mathbf{i} and \mathbf{j} satisfying (12) we have:

$$\begin{aligned} \mathbf{p}_1^T \mathbf{i} = \mathbf{p}_2^T \mathbf{j} &\Rightarrow \mathbf{p}_1^T A\mathbf{r} = \mathbf{p}_2^T B\mathbf{r} \\ \mathbf{p}_1^T A &= \mathbf{p}_2^T B \end{aligned} \quad (13)$$

(13) can be satisfied if and only if the row spaces of A and B intersect, as the LHS of the (13) is a linear combination of the rows of A , while the RHS is a linear combination of the rows of B . We now consider the problem that arises when comparing two images taken of the same 3D scene (face) from different viewpoints. This raises problems of finding a correspondence between pixels in the two images, as well as accounting for occlusion. To work our way up to this problem, we first consider the case in which there exists a one-to-one correspondence between pixels in the image, with no occlusion.

Permutations: In this case, we can suppose that A is the identity matrix and B is a permutation matrix, which changes the location of pixels without altering their intensities. Thus, A and B are both of full rank, and in fact they have a common row space. So, there exist \mathbf{p}_1 and \mathbf{p}_2 that will project \mathbf{i} and \mathbf{j} into a space where they are equal.

Stereo: We now consider a more general problem that is commonly solved by stereo matching. Suppose we represent a 3D object with a triangular mesh. Let \mathbf{r} contains the intensities on all faces of the mesh that appear in either image (We will assume that each pixel contains the intensity from a single triangle. More realistic rendering models could be handled with slightly more complicated reasoning). Then, to generate images appropriately, A and B will be matrices in

which each row contains one 1 and 0 otherwise. A (or B) may contain identical rows, if the same triangle projects to multiple pixels. The rank of A will be equal to the number of triangles that create intensities in \mathbf{i} , and similarly for B . The number of columns in both matrices will be equal to the number of triangles that appear in either image. So their row spaces will intersect, provided that the sum of their ranks is greater than or equal to the length of \mathbf{r} , which occurs whenever the images contain projections of any common pixels. As a toy example, we consider a small 1D stereo pair showing a dot in front of a planar background. We might have $\mathbf{i}^T = [7\ 8\ 2\ 3\ 5]$ and $\mathbf{j}^T = [7\ 2\ 3\ 5]$. In this example we might have $\mathbf{r}^T = [7\ 8\ 2\ 3\ 5]$ and

$$A = \begin{pmatrix} 1 & 0 & 0 & 0 & 0 \\ 0 & 1 & 0 & 0 & 0 \\ 0 & 0 & 1 & 0 & 0 \\ 0 & 0 & 0 & 0 & 1 \end{pmatrix} \quad B = \begin{pmatrix} 1 & 0 & 0 & 0 & 0 \\ 0 & 0 & 1 & 0 & 0 \\ 0 & 0 & 0 & 1 & 0 \\ 0 & 0 & 0 & 0 & 1 \end{pmatrix}$$

It can be inferred from the example that row spaces of A and B intersect hence we expect the CLS framework to work.

4.2. Partial Least Square based CLS

A Partial least square based framework learns projectors for every pair of gallery and probe poses using a training set of subjects appearing in roughly the same gallery/probe pose pairs. Let us denote gallery and probe poses as g and p respectively. Let X_g ($d_g \times N$) and X_p ($d_p \times N$) be the data matrices with columns as mean subtracted image vectors in pose g and p respectively with d_g and d_p as gallery and probe image dimensions and N is the number of training subjects. PLS finds projectors W_g ($d_g \times K$) and W_p ($d_p \times K$) with $K = \#$ PLS factors for pose g and p , such that

$$\begin{aligned} X_g &= W_g T_g + R_g \\ X_p &= W_p T_p + R_p \\ T_p &= D T_g + R \end{aligned} \tag{14}$$

Here, T_g ($K \times N$) and T_p ($K \times N$) are the latent projections of images in the CLS, R_g ($d_g \times N$), R_p ($d_p \times N$) and R ($K \times N$) are residual matrices in appropriate spaces and D is a diagonal matrix that scales the latent projections of gallery images to make it equal to the probe image's projection in the latent space. Fig2 depicts the PLS framework pictorially. The detailed step by step algorithm to obtain these variables is given in [20].

4.3. PLS on CMU PIE

The PLS based framework is used for pose invariant face recognition on CMU PIE dataset which has been used by many researchers previously for evaluation. This dataset contains 68 subjects in 13 different poses and 23 different illumination conditions. We took subjects from 1 to 34 for training and the remaining 35 to 68 for testing. As we are dealing with pose variation only, we took all the images in frontal illumination which is illumination 12. As a preprocessing step, 4 fiducial points (both eyes center, nose tip and mouth) were hand

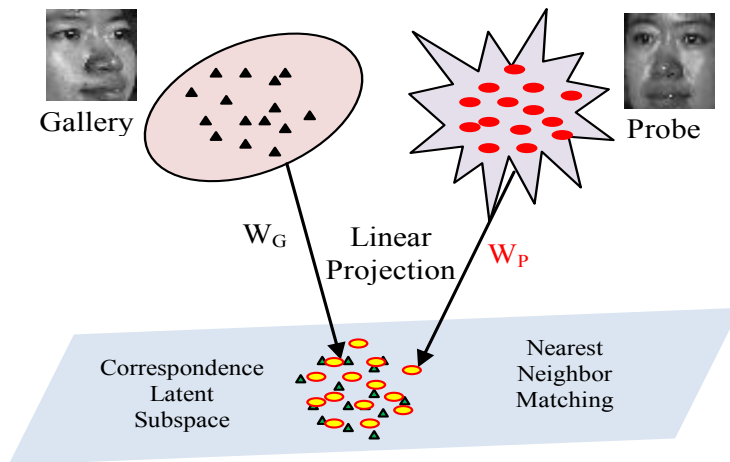


Figure 2: PLS based framework for pose invariant face recognition, W_g and W_p are learned using PLS and training images in gallery and probe pose.

Table 1: CMU PIE accuracy using 1-NN matching and PLS with 30 dimensional CLS overall accuracy is **90.08**

Probe→ Gallery↓	c34	c31	c14	c11	c29	c09	c27	c07	c05	c37	c25	c02	c22	Avg
c34	-/-	88.0	94.0	94.0	91.0	88.0	91.0	97.0	85.0	88.0	70.0	85.0	61.0	86.2
c31	85.0	-/-	100.0	100.0	100.0	88.0	85.0	91.0	85.0	88.0	76.0	85.0	76.0	88.4
c14	97.0	100.0	-/-	100.0	97.0	91.0	97.0	100.0	91.0	100.0	82.0	91.0	67.0	92.8
c11	79.0	97.0	100.0	-/-	100.0	88.0	100.0	100.0	97.0	97.0	85.0	88.0	67.0	91.6
c29	76.0	94.0	100.0	100.0	-/-	100.0	100.0	100.0	100.0	100.0	85.0	91.0	73.0	93.3
c09	76.0	88.0	91.0	94.0	94.0	-/-	97.0	94.0	91.0	88.0	82.0	79.0	70.0	87.2
c27	85.0	91.0	97.0	100.0	100.0	100.0	-/-	100.0	100.0	100.0	85.0	88.0	79.0	93.9
c07	79.0	91.0	97.0	100.0	100.0	97.0	100.0	-/-	100.0	97.0	85.0	91.0	76.0	92.9
c05	79.0	97.0	97.0	94.0	100.0	94.0	100.0	100.0	-/-	97.0	91.0	91.0	82.0	93.6
c37	79.0	94.0	100.0	94.0	94.0	88.0	94.0	94.0	97.0	-/-	100.0	100.0	94.0	94.1
c25	67.0	82.0	76.0	79.0	88.0	88.0	88.0	91.0	94.0	97.0	-/-	97.0	76.0	85.5
c02	76.0	88.0	88.0	94.0	94.0	88.0	97.0	94.0	100.0	100.0	100.0	-/-	97.0	93.1
c22	64.0	70.0	64.0	79.0	76.0	67.0	82.0	82.0	85.0	91.0	85.0	91.0	-/-	78.4

annotated and an affine transformation was used to register the faces based on the fiducial points. After all the faces are aligned in corresponding poses we cropped 48×40 facial region. Images were turned into gray-scale and direct intensity values mapped between 0 to 1 were used as features. The number of PLS factors was set to be 30. Choosing more than 30 did not affect the performance but choosing less than 30 worsens the performance. The resulting CLS framework was termed as PLS³⁰, indicating 30 dimensional CLS obtained using PLS. The accuracy for all possible gallery-probe pairs is given in Table 1. For comparing our approach with other published works we calculated the average of all gallery-probe pairs and the resulting accuracy is listed in Table 2. Some authors have reported their results on CMU PIE data with only frontal pose as gallery and a subset of non-frontal poses as probe. For comparison we also list the gallery and probe setting in Table 2. A simple comparison clearly reveals that PLS³⁰ approach outperforms all the methods.

Table 2: comparison of PLS with other published work on CMU PIE.

Method	Gallery/Probe	Accuracy	PLS ³⁰
Eigenface [33]	all/all	16.6	90.1
ELF [33]	all/all	66.3	90.1
FaceIt [33]	all/all	24.3	90.1
4ptSMD [31]	all/all	86.8	90.1
SlantSMD [32]	all/all	90.1	90.1
Ridge [38]	c27/rest all	88.24	93.9
Yamada [22]	c27/rest all	85.6	93.9
LLR [12]	c27/c(05,07,09,11,37,29)	94.6	100
PGFR [44]	c27/c(05,37,25,22,29,11,14,34)	86	93.4
<i>Gabor</i> [38]	<i>c27/rest all</i>	<i>90.9</i>	<i>93.9</i>

4.4. Performance drop on FERET and MultiPIE

In this subsection, we first show the results of PLS based framework on FERET and MultiPIE datasets and discuss the reason behind the poor performance. Subsequently, based on the studies we propose our extended two-stage discriminative approach followed by a detailed analysis of model parameters on the overall performance.

The performance of PLS based approach on FERET and MultiPIE dataset is shown in Fig8(a) and Fig8(b), respectively. From the figures it is evident that performance has decreased significantly for both MultiPIE and FERET. The most obvious reason is the increased size testing subjects (gallery); FERET and MultiPIE have almost 3 and 7 times as many testing subjects as compared to CMU PIE, respectively. As the number of testing subjects increases, we need discriminative representation for effective classification. All three i.e. CCA, BLM and PLS are generative in nature, hence, the decline in accuracy with increasing number of testing subject is natural. It suggests the use of discriminative representation for better performance. Secondly, we noticed that some of the faces in the dataset were off by few degrees from the reported pose in the dataset. Especially for FERET, [5] has reported estimated poses which are very different from the ground-truth poses supplied with the dataset. Since, we use images from FERET and MultiPIE to learn projectors, it leads to pose difference between the projectors and images. We term this phenomenon as *pose error*. It can occur because of head movement during acquisition or wrong pose estimation. Suppose, we learn two projectors for a $0^\circ/30^\circ$ gallery/probe pose pair. Let us assume that the 30° testing images are not actually 30° but $(30 \pm \theta)^\circ$ with $\theta \in [0, 15]$. For $\theta \leq 5$, the projectors and the testing images will have sufficient pixel correspondence. But for $\theta \geq 5$, we again face the loss of correspondence, resulting in poor performance. Pose errors are inevitable and present in real-life as well as controlled conditions which is evident from FERET and MultiPIE. Moreover, due to different facial structures we may expect loss of correspondence for pose angles greater than 45° . For example, both the eyes of Asians are visible even at a pose angle of around 60° because of relatively flat

facial structure as compared to European or Caucasian for which the second eye becomes partially or totally occluded at 60° . This leads to missing facial regions at large pose angles which creates loss of correspondence. These pose errors become more frequent and prominent with increasing pose angles.

4.5. Pose estimation

In order to show that the poses provided in the FERET and MultiPIE databases are inaccurate, we assume that for each subject the frontal pose is correct and use this information to estimate the non-frontal poses; the change in the distance between the eyes of the subject, with respect to the distance in frontal pose, is used to calculate the new pose. In general, the change in the observed eye distance can be due to two factors: change in pose and/or change in the distance between the camera and the face. For the change in the face-camera position, the distance between the nose and the lip can be used to correct this motion, if present. For the pose change, in the two datasets, there is negligible change in yaw and the Euclidean distance automatically correct for any roll change, i.e. in-plane rotation; therefore, the Euclidean eye distance once corrected by the nose-lip distance can be directly used to measure the pitch pose.

The distance between the two eyes in frontal pose will be denoted by ee_1 and the distance between the nose and the lip by nl_1 ; similarly for the non-frontal pose to be estimated, the distance between the eyes is given by ee_2 and that between the nose and lip by nl_2 . Assuming that the eyes, nose and lip are coplanar, i.e. the effect due to the nose sticking out is negligible, the new pose θ can be calculated as: $\theta = \arccos(\frac{ee_2/nl_2}{ee_1/nl_1})$. A pictorial demonstration of this calculation is shown in Fig 3.

To measure the poses in FERET and MultiPIE, manually annotated images were used to obtain the fiducial points and the frontal pose was used to calculate the rest of the non-frontal poses as explained above. The box and whisker plots for the estimated pose vs. the ground-truth pose for FERET and MultiPIE are shown in Fig 4 and Fig 5, respectively. It is clear that, in both databases, there are inconsistencies between the different subjects at the same pose, rendering

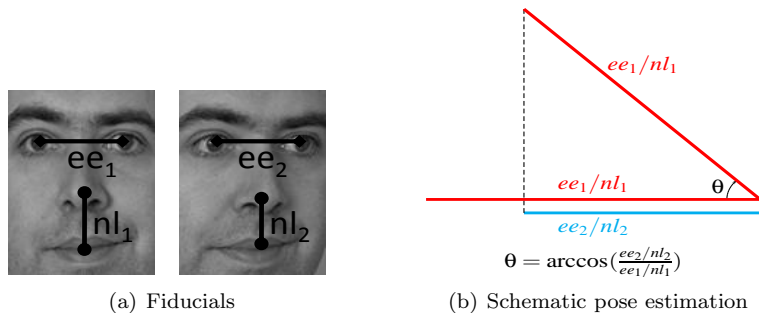


Figure 3: Schematic diagram to estimate the pose of a non-frontal face using fiducials.

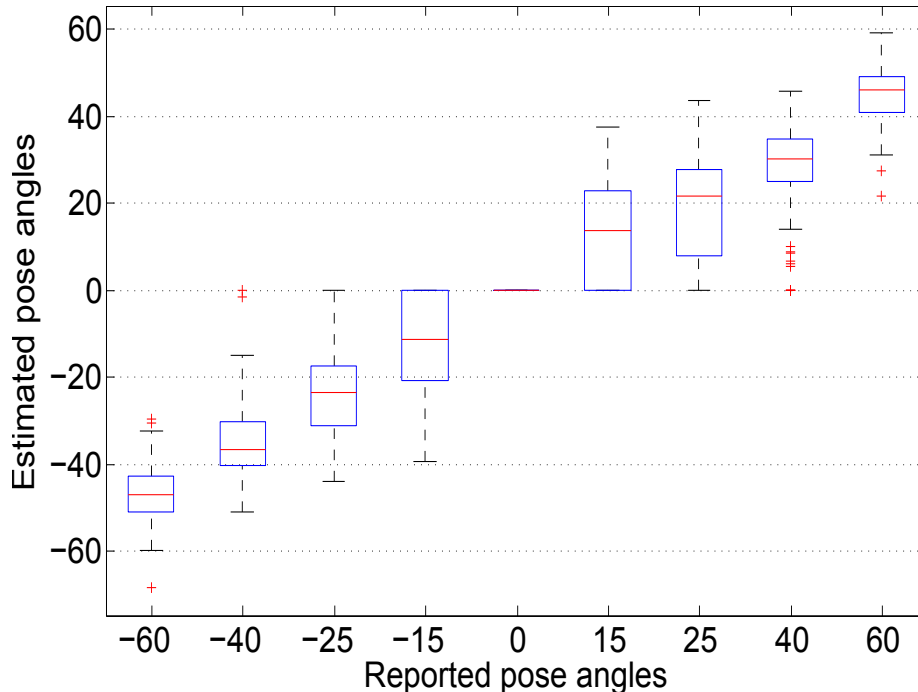


Figure 4: Box and Whisker plot for pose errors on FERET data for all the 9 poses.

both ground truth data inaccurate. The pose errors are higher in magnitude and scatter in FERET which is obtained under unconstrained conditions as compared to MultiPIE.

4.6. Two-stage Discriminative Correspondence Latent Subspace

A discriminative representation approach such as LDA, requires multiple images per sample to learn the discriminative directions. We have a training set containing multiple images of a person but all the images are in different poses. Due to the loss of feature correspondence, we cannot use these multi-pose images directly to learn LDA directions. Results in [12] show that directly using them will lead to poor performance. However, we can learn a CLS for more than two poses simultaneously such that the projections of different pose images in the latent space have correspondence. Now, the multiple latent projections of a person can be used with LDA. Fortunately, using CCA as in Eqn3, we can learn projectors for multiple poses to get a common CLS for a set of multiple poses. We empirically found that just using judiciously chosen set of poses (without LDA in latent space) to learn projectors offers some improvement over using only two poses. We defer the detailed discussion to later sections. The multiple pose approach without LDA in latent space is termed Multiple CLS or MCLS and with LDA is termed Discriminative MCLS or DMCLS. The latent space projection \mathbf{x}_l^i of i^{th} subject in pose p (\mathbf{x}_p^i) is give as

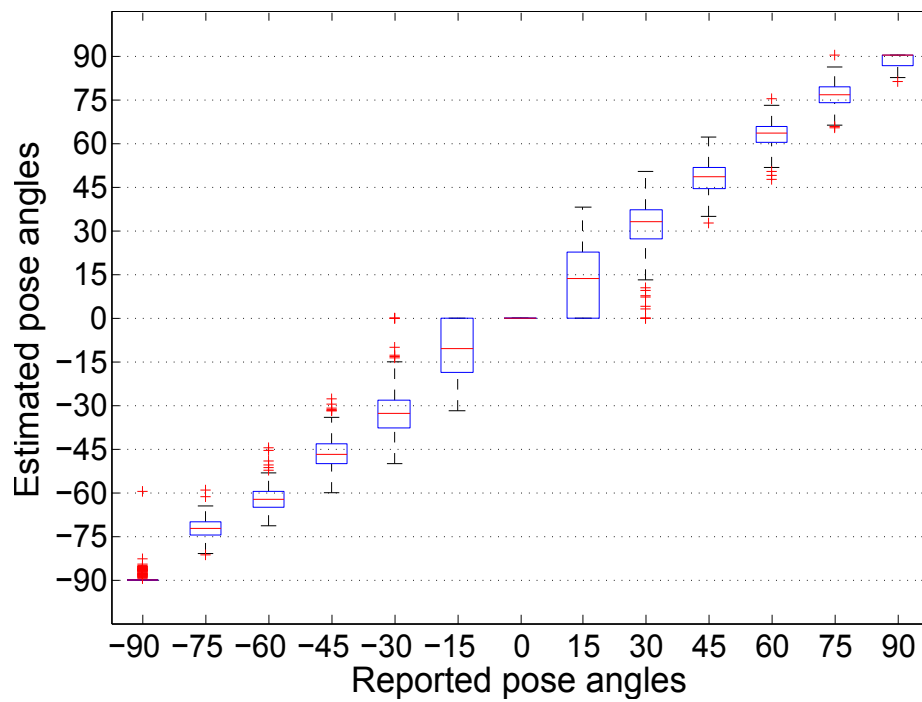


Figure 5: Box and Whisker plot for pose errors on MultiPIE data for all the 13 poses which have only pitch variation from frontal.

$$\mathbf{x}_l^i = W_p^T \mathbf{x}_p^i \quad (15)$$

Here, W_p^T is the projector for pose p and the subscript l indicates that \mathbf{x}_l^i is in latent space. The projections of images in pose p using a projector for pose p are termed *same pose projections*. The latent space LDA offers discrimination based on the identity which is shown to be effective for classification [10, 7].

The performance drop study also suggests that pose error is an important factor and needs to be handled for better performance. To tackle the pose error, we draw motivation from [9, 43, 8] where it has been shown that the inclusion of expected variations (in the testing set) in the training set improves the performance. Specifically, [9] has shown that using frontal and 30° training images with LDA improves the performance for 15° testing images. And, [8] shows that using artificially misaligned images, created by small random perturbation of fiducial points in frontal pose, during training with LDA offers robustness to small errors in fiducial estimation. We combine the two approaches and artificially simulate pose errors. Unfortunately, creating small pose errors is not as simple as creating fiducial misalignment in frontal images. We do it by deliberately projecting face images onto adjacent pose projector to obtain *adjacent pose projections*. The dataset used has pose angle increments in steps of 15° ; therefore, projection of 45° image onto 30° and 60° projectors will give adjacent pose projections for 45° . The set of adjacent projections is given by

$$\mathcal{X}_l^i = \{\tilde{\mathbf{x}}_l^i : \tilde{\mathbf{x}}_l^i = W_{q \in A(p)}^T \mathbf{x}_p^i\} \quad (16)$$

here, $A(p)$ is the set of adjacent poses for pose p . The use of adjacent pose projections with LDA is expected to offer some robustness to small pose errors.

Same and adjacent pose projections have complimentary information and both are important for robust pose-invariant face recognition. Therefore, we use both of them together as training samples with LDA to learn a discriminative classifier in the latent space. We call the resulting framework: Adjacent DMCLS or ADMCLS. ADMCLS is expected to offer robustness to pose errors smaller than 15° which is indeed the general range of pose errors observed in real-life as well as controlled scenario. Apart from providing robustness to pose error, adjacent projection also provide more samples per class for better estimation of class mean and covariance. We empirically found that inclusion of pose error projections dramatically improves the performance on FERET and MultiPIE which is in accordance with [8] and our intuition. It also supports our claim that performance drop is due to pose errors. The complete flow diagram for the ADMCLS framework is depicted in Fig.7.

4.7. Parameters and their effect

The proposed ADMCLS framework is basically a two stage approach. The first stage involves learning the CLS and the second stage is learning the LDA directions using the projections in the latent subspace. Both stages have several different parameters and variation in these parameters will lead to different

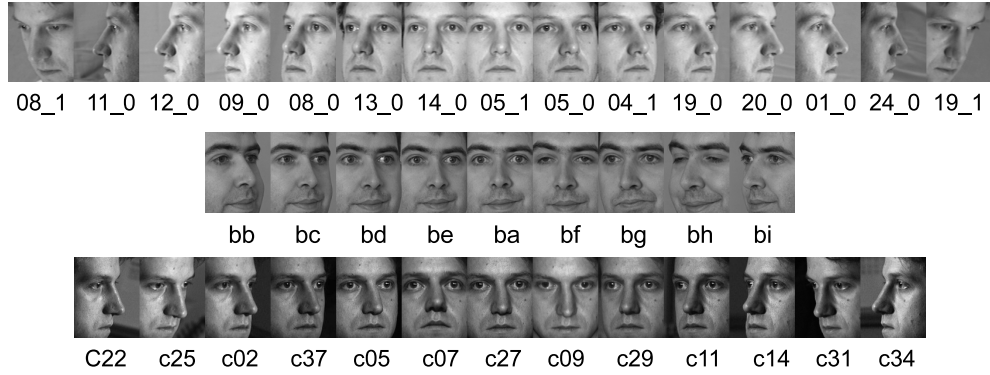


Figure 6: Images with pose names, **MultiPIE** (top row), **FERET** (middle row) and **CMU PIE** (bottom row).

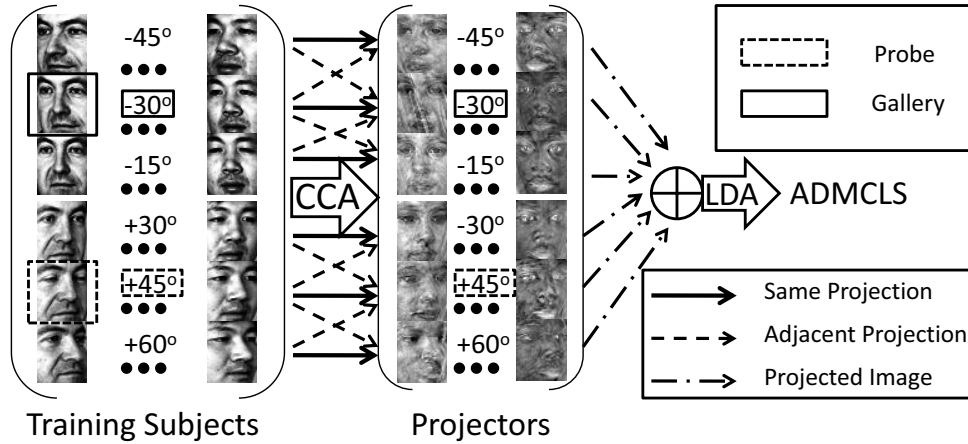


Figure 7: The flow diagram showing the complete ADMCLS process pictorially for a pair of gallery (-30°) and probe ($+45^\circ$) pose pair. The gallery and probe along with adjacent poses constitute the set of poses for learning the CLS ($\pm 30^\circ$, $\pm 45^\circ$, -15° and $+60^\circ$ for this case). Once the CLS is learned, same and adjacent pose projections (indicated by different arrow type) are carried out to obtain projected images in the latent subspace. An arrow from pose p images to pose q projector means projection of pose p images on pose q projector. All the projected images of a particular subject are used as samples in latent space LDA.

overall framework. In this subsection we discuss the involved parameters and their effect on overall performance. We also discuss various criteria to choose these parameters and their effect on the final performance.

To test the effect of a parameter, all the others were kept fixed and only the parameter in question was varied. Then the best values of individual parameters are combined to give the final framework. The final accuracy of the system is used as the performance measure for each parameter. To maintain consistency, reproducibility and to facilitate comparison of our approach with others in the future we have fixed the training subjects to be subject ID 1 to 34 for CMU PIE, 1 to 100 for MultiPIE and 1 to 100 (when arranged according to name) for FERET. Testing is done on the rest of the subjects i.e. 34, 237 and 100 testing subjects for CMU PIE, MultiPIE and FERET respectively.

4.7.1. Latent Subspace Dimension and Learning Model

This is an important parameter in all the subspace based methods and plays a critical role in performance. Too many dimensions can lead to over-fitting and too few to under-fitting; therefore, this parameter needs to be decided very carefully. There are some techniques based on the spectral energy of the eigen-system that can guide the proper selection such as: choosing a pre-defined ratio of energy to be preserved in the selected number of dimensions. In the case of CCA, we selected top k eigen-vectors. We will see later that our final framework does not require a very careful selection of this parameter and is pretty robust to its variation. In the case of PLS we are using an iterative greedy algorithm and the number of dimensions can be selected by using only those directions which contain some pre-specified amount of total variation. However, it was observed that beyond a certain number of dimensions the accuracy remains constant. For BLM, we can use the spectral energy approach to select the number of dimensions. The selected number of dimensions of the CLS would be indicated as a superscript of the final framework name.

To keep things simple we have used 2 poses and 1-NN matching as the constituents of the final framework and varied the number of dimensions of CLS. The accuracy is the average accuracy for all possible gallery-probe pairs for the same number of CLS dimensions. There are 15 poses in MultiPIE so there is a total of 210 gallery-probe pose pairs and 72 for FERET (9 poses). The variation of accuracy for PLS, CCA and BLM on FERET and MultiPIE is shown in the Fig.8(a) and Fig. 8(b). It is obvious that different gallery-probe pairs will achieve the maximum accuracy with different number of CLS dimensions but we are calculating the average accuracy by considering the same CLS dimension for all pairs. To show the difference between our performance measure and the best possible accuracy obtained by using different CLS dimensions for different gallery-probe pairs, we calculated the best accuracy for all the pose pairs and averaged them to get the overall accuracy. These best accuracies are plotted as dashed horizontal lines in the same figure.

The learning model has significant impact on the overall performance. We investigated three different choices for learning method: CCA, PLS and BLM and found that PLS performed slightly better than CCA for pose invariant face

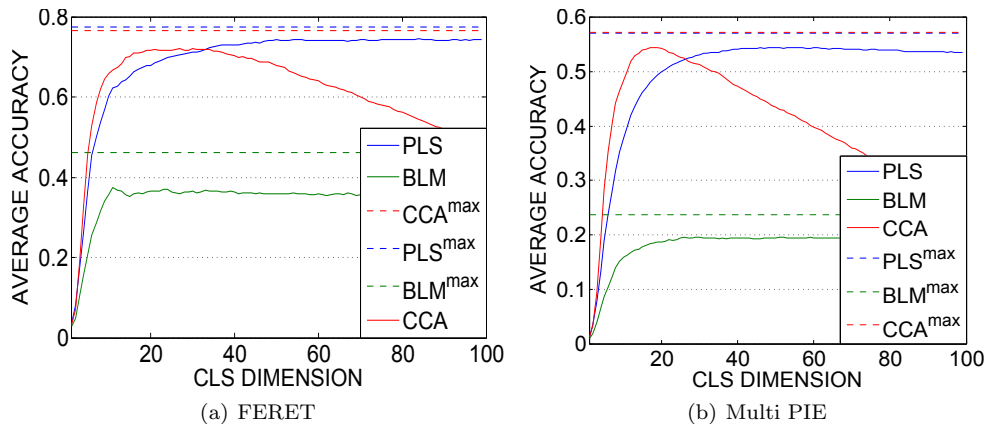


Figure 8: Result of CLS based recognition using 1-NN classifier on FERET and MultiPIE. $(CCA/PLS/BLM)^{max}$ represents the maximum possible accuracy using different number of CLS dimensions for all gallery-probe pairs.

recognition and BLM is the worst performing [11]. However, PLS cannot be used to learn a CLS framework for more than two poses which makes it useless for the MCLS framework and BLM performs significantly worse than CCA. So, we used CCA for the cases when more than two poses are used for training.

Fig.10 clearly reveals the difference between different learning models and some interesting observations. The most important and satisfying observation is that the maximum possible accuracy is not significantly higher than the average accuracy justifying our assumption of equal CLS dimension across all gallery/probe pose pairs. Clearly, BLM performance is significantly worse than CCA and PLS which is in accordance with the results obtained in [11]. The performance of CCA and PLS is almost similar for MutliPIE and PLS performs better than CCA for FERET which is also in accordance with [11]. One clear observation from the figure is that CCA performance is sensitive to CLS dimension and achieves maxima in a short range. On the other hand, the performance of BLM and PLS increase till a certain number of dimensions and then stays nearly constant. This brings out the fact that CCA is prone to over fitting while BLM and PLS are not.

4.7.2. Set of training poses

This has some effect on the obtained projectors since different sets of training poses will generate somewhat different projectors for each pose pair. Moreover, the supervised classifier in the latent space uses the projections as samples hence, it will have some bearing on the classifier too. In the case of PLS learning model, we can have only 2 training poses because of the inability of SIMPLS algorithm to learn more than 2 poses simultaneously but this is not a problem for BLM and CCA. The set of poses used for training has deep impact on the obtained CLS performance and further improvements. We indicate the use of multiple

training poses in the framework by preceding CLS by M i.e. MCLS.

The intuition of using more than two training poses can be understood in terms of robustness to noise offered by additional poses for CCA. It was pointed out and proved in [30], in a completely different context of clustering that adding more styles of data improves noise-robustness which also holds in our case of pose variation. As explained earlier in sub-section 3.2, CCA based CLS is a way of learning correspondence by maximizing correlation. The correlation between the training images in two different poses are most likely due to two factors - true correspondence and noise. We ideally want that the correlation is only due to correspondence. However, our data always contains some noise in the form of pose errors and/or inaccurate fiducial location. Presence of noise in the data can cause spurious correlations leading to false correspondence which will affect the performance. When more than two poses are used simultaneously, the obtained correlation between these poses has a higher probability to be due to correspondence because it is present in all the poses. However, this does not mean that we should add too many poses because it will decrease the flexibility of the learning model leading to under-fit. Two poses will lead to over-fitting and too many will cause under-fitting hence we choose 4 poses to strike a balance.

To evaluate the effect of changing the sets of training poses on the final framework for a particular gallery-probe pair, we include poses other than gallery and probe poses to learn CLS. This procedure raises some interesting questions: Which poses should be included in training set? how many poses should be used? To answer these questions, we adopt a very simple approach that illustrates the effect of using multiple training poses. We use three gallery poses and all the possible probe poses for those three. For FERET we choose pose **ba**(frontal), **bd** (25°) and **bb** (60°) and for MultiPIE we choose 051(frontal), 190(45°) and 240(90°) as gallery poses. In addition to the gallery and probe we also select adjacent intermediate poses based on the viewing angle i.e. if we have gallery as frontal (0°) and probe as $+60^\circ$ then we take two additional poses to be $+15^\circ$ and $+45^\circ$. Similarly, for gallery as frontal and probe as $+30^\circ$ we take only one additional pose $+15^\circ$ since it is the only intermediate pose.

Once the latent subspace is learned we use 1-NN for classification. The number of CLS dimensions is kept at 17 so the final frameworks are called as MCLS¹⁷. We show the comparison of MCLS¹⁷ vs. CCA²⁰ in Fig.10(a) and Fig.10(b) for FERET and MultiPIE respectively. There are some missing points in the performance curves in both figures because an adjacent gallery-probe pose pair does not have any intermediate pose. The comparison clearly highlights the improvement offered by using multiple poses for learning the latent subspace. We especially observe a significant increase in accuracy with MCLS¹⁷ framework for gallery and probe poses with large pose difference except for few places where it either remains the same or decreased slightly. We also observe that the improvement is more significant in FERET as compared to MultiPIE which is due to the fact that MultiPIE dataset has less pose errors than FERET as shown in subsection IV.E. Therefore, MCLS framework has more to offer in terms of robustness to pose errors in FERET as compared to MultiPIE.



Figure 9: Projector bases corresponding to top eigen-values obtained using CCA (first 5 rows) and PCA (bottom 5 rows) obtained using 100 subjects from FERET. CCA projectors are learned using all the poses simultaneously and PCA projectors are learned separately for each pose. Each row shows the projector bases of the pose for equally indexed eigen-value. Observe that, projector bases are hallucinated face images in different poses and the CCA projector bases look like rotated versions of the same hallucinated face but there is considerable difference between PCA projectors. This picture visually explains the presence of correlation in the latent CLS space using CCA and its absence using PCA.

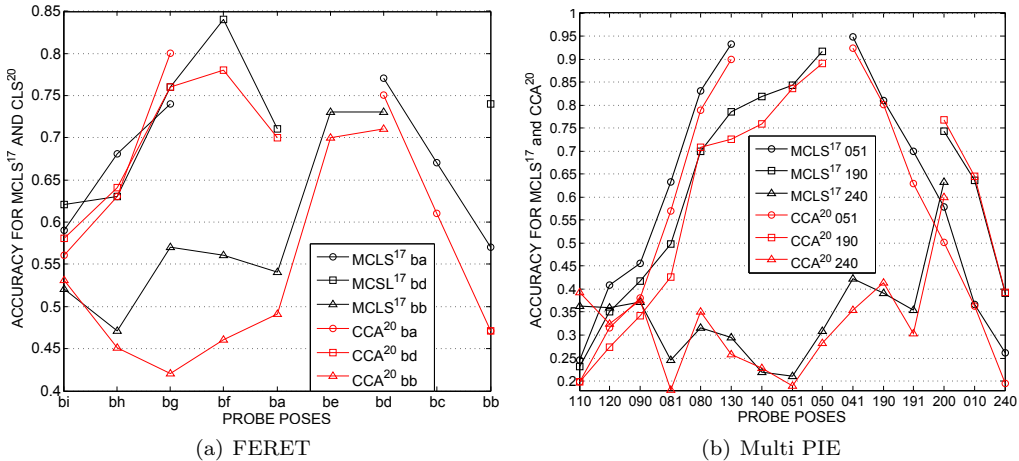


Figure 10: Comparison of $MCLS^{17}$ vs. CCA^{20} with varying gallery-probe pairs for a) three gallery poses ba(frontal), bd(40°) and bb(60°) on FERET dataset. b) Three gallery poses 051(frontal), 190(45°) and 240(90°) on MultiPIE dataset. $MCLS^{17}ba$ indicates that the gallery is pose **ba**, **multiple** poses are used during training and CCA is the learning model with **17** dimensional CLS and **1-NN** classifier while $CCA^{20}ba$ indicates that the gallery is pose **ba**, **two** poses are used during training and **CCA** is the learning model with **18** dimensional CLS and **1-NN** classifier

The second stage of the framework is learning a supervised classifier using the latent subspace projections. This stage has two crucial parameters:

4.7.3. Set of projections and Classifier

It refers to the combination of the set of latent subspace projections for a person and the classifier used for matching. As discussed already, we have two choices for projecting a face image in the CLS and both contain complimentary information which can be utilized by the classifier for recognition. Since all the databases used in this paper have pose angles quantized in steps of 15° , the difference between any two adjacent poses is 15° . In our framework, do not consider more than 15° pose difference because they will render the projection meaningless and they do not exist in real life scenario.

As mentioned earlier that CCA is used as the learning model for all the experiments with more than two poses in the training. MultiPIE has 15 poses and FERET has 9, so the size of the eigen-system for MultiPIE becomes too big and requires large memory. So, all the exploratory experiments were done with FERET and conclusions were used to decide the optimal strategy for MultiPIE. In order to avoid under-fitting we adopt a simple strategy to select a subset of poses for training which is based on gallery-probe pair. The gallery-probe pairs along with the adjacent poses of them are selected as the training set of poses. So, for a $+45^\circ / -30^\circ$ gallery/probe pair the training set would be $\pm 30^\circ, \pm 45^\circ, +60^\circ, -15^\circ$ and for $-15^\circ / 0^\circ$ training pose set is $\pm 15^\circ, 0^\circ, 30^\circ$. Adjacent poses are selected to simulate pose error scenario. We call this variant

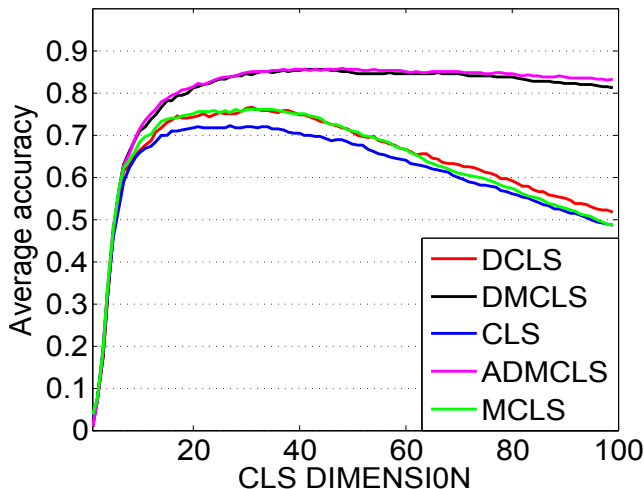


Figure 11: Variation of CLS, MCLS, DCLS, DMCLS and ADMCLS accuracy with latent space dimension for all the gallery-probe pairs on FERET.

of DMCLS as Adjacent Discriminant Multiple Coupled Subspace or ADMCLS. To evaluate the effect of latent space projections, we plot the average accuracy across all 72 gallery/probe pairs in Fig. 11 for the following settings: 1-NN classifier with two poses i.e. CLS; Intermediate poses and 1-NN classifier i.e. MCLS; two poses and LDA i.e. DCLS; all 9 poses for FERET and adjacent projections with LDA i.e. DMCLS and adjacent set of training poses with adjacent projections and LDA i.e. ADMCLS.

It is clear from the Fig.11 that ADMCLS performed best closely followed by DMCLS, while, CLS showed the worst performance with DCLS and MCLS performing slightly better. The use of LDA with adjacent projections did not only increase the accuracy significantly but also was fairly insensitive to CLS dimension which eliminates the burden of determining it by cross-validation. This significant improvement is due to artificial simulation of pose error scenarios and learning to effectively neglect such misalignments for classification using LDA. One more reason contributing to the improvement is the LDA assumption of similar within-class covariance for all the classes. In our case, indeed the within-class covariance matrices are almost the same because the samples of all the classes in CLS are obtained using same set of CLS bases and the types of projection are also the same for all the classes. The recognition rates for all the 72 pose pairs with DMCLS⁴⁰ using all the pose pairs in training set are given in Table 4. To prove the point that the improvement is actually due to handling pose errors we also obtain the relative improvement by ADMCLS⁴⁰ over CLS²² for all gallery-probe pairs. The difference is plotted as a heat map for better visualization in the Fig.12(a). From the figure, it is evident that the most significant improvements are in the cases where either the gallery or the probe pose is far away from frontal pose. In these cases, the chance and extent

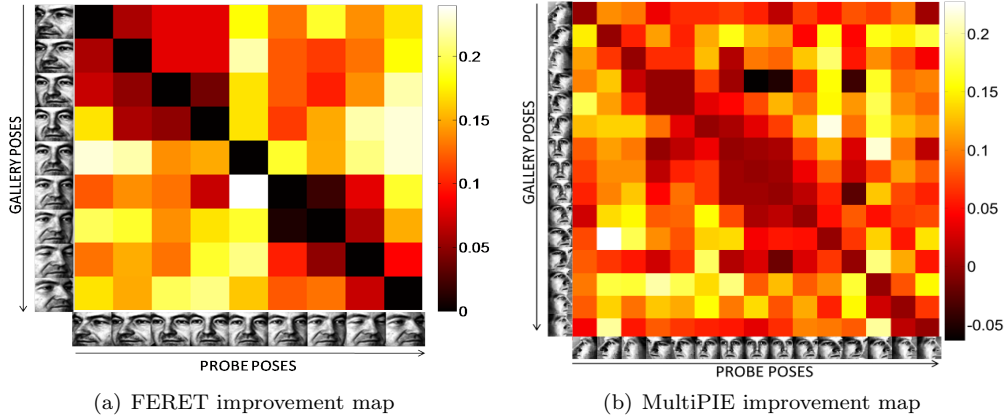


Figure 12: Improvement map for (a) using ADMCLS⁴⁰ over CCA²⁰ for FERET and (b) using ADMCLS²⁵ over CCA¹⁸ for MultiPIE. The original accuracies were all between 0 (0%) and 1 (100%). It is evident from the two maps that the amount of improvement is more in FERET as compared to MultiPIE. Also, the improvement is more when either the gallery or probe pose is far from the frontal view.

Table 3: Framework names based on the components used, the super-script in the name denotes the CLS dimension.

Name	Model	Training Set Poses	Projections	Classifier	CLS Dimension
CCA ¹⁰	CCA	gallery + probe	same pose	1-NN	10
PLS ¹⁰	PLS	gallery + probe	same pose	1-NN	10
BLM ²⁰	BLM	gallery + probe	same pose	1-NN	20
MCLS ¹⁰	CCA	gallery + probe + Intermediate	same pose	1-NN	10
DMCLS ⁴⁰	CCA	all poses	same + adjacent pose	LDA	40
ADMCLS ¹⁰	CCA	gallery + probe + adjacent	same + adjacent pose	LDA	10

of pose errors and incorrect fiducial locations is most likely and prominent.

Owing to the block structure of the proposed approach there are various different frameworks possible that gives rise to different names. For the ease of understanding and readability we define all the names and the components used in the Table 3.

5. Experimental Analysis

In this section we provide the final results obtained on CMU PIE, FERET and MultiPIE using the proposed approach and compare our results with prior work on the same datasets. Please note that, CCA is used as learning model for all the methods using more than two poses in training set, for reasons explained in previous sections.

5.1. Training and Testing Protocol

Like any other learning based approach we require training data to learn the model parameters. We assume access to a training data that has multiple

images of a person under different poses and ground-truth poses of training as well as testing faces. Although fiducial points can be used for a better estimation of pose, we use the ground-truth poses for a fair comparison with previous approaches. Moreover, automatic pose estimation algorithms and fiducial detectors always have some error. Therefore, working with small pose errors reflects performance with automatic pose or fiducial detector. CMU PIE, FERET and MultiPIE have multiple images of a person under a fixed set of poses. Hence, we use some part of the data as training and the rest as testing. We also need to align the faces under different poses which requires fiducial landmark points. In the training phase, we obtain the projectors for all the possible gallery/probe pose pairs for the required framework i.e. ADMCLS, DMCLS etc. At testing time, we assume that the gallery and probe poses are known and use appropriate projectors for projection followed by matching. For testing purpose we always project the images on the same pose projector as per as the ground-truth poses. For a completely automatic face recognition system, pose and fiducial landmarks should be obtained automatically. However, for experimentation purposes, we assume them to be known beforehand, a common practice followed in many papers [14, 15, 38, 22, 12, 33, 39, 2, 40, 13, 9]. Fortunately, research and commercial systems have shown impressive performance in automatic pose and fiducial determination which can be used in conjunction with our approach to make an automatic pose invariant face recognition system.

5.2. FERET

This dataset contains 200 subjects in 9 different poses spanning $\pm 60^\circ$ viewpoint. All the images for one person along with the pose name are shown in Fig.6. Pre-processing steps similar to CMU PIE were used except that the final facial region crops are of size 50×40 pixels. Subjects 1 to 100 were chosen as training subjects and 101 to 200 as testing. Since, there are 9 poses, we have 72 different gallery-probe pairs. We report the accuracy for FERET data set using two different variants of DMCLS for bringing out the fact that using more than required number of poses in training may lead to poor performance. We report DMCLS based accuracy which uses all the 9 poses in the training and adjacent projection based LDA in latent space and ADMCLS based accuracy which uses a subset of poses for training. Once again the number of CLS dimension is indicated as the superscript and CCA is used as the learning model. Table 4 reports the accuracy for all possible gallery-probe pairs using the two different variant i.e. DMCLS and ADMCLS. The table clearly indicates the advantage of using ADMCLS over DMCLS when near frontal poses are used as gallery pose. It also indicates that when extreme poses are gallery then using DMCLS is slightly better than ADMCLS, a possible explanation could be the fact that extreme poses require more regularization than flexibility. We report the accuracy obtained using 3DMM [5] approach to indicate the performance difference between 2D and 3D approaches. The difference between 2D and 3D approaches supports the fact that 3D information improves performance in pose invariant face recognition. We have shown the result of [38] under two settings i.e. with and without Gabor features. The authors have extracted Gabor features at

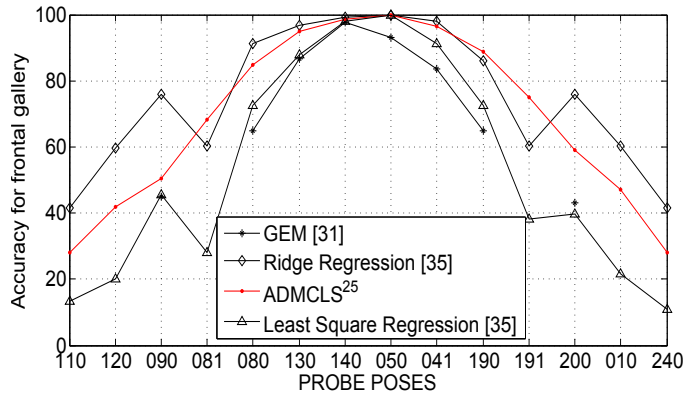


Figure 13: Comparison of $ADMCLS^{25}$ with other approaches on MultiPIE dataset with frontal gallery.

Table 4: $DMCLS^{40}/ADMCLS^{40}$ for all possible gallery-probe pairs on FERET

Pose Angle	bi -60°	bh -40°	bg -25°	bf -10°	ba 0°	be 10°	bd 25°	bc 40°	bb 60°	$DMCLS^{40}$ Avg/ $ADMCLS^{40}$ Avg
bi	-/-	98/98	92/93	88/82	70/77	81/80	79/80	76/69	70/63	81.75 /80.25
bh	97/97	-/-	99/99	94/94	80/84	90/87	79/77	71/70	62/60	84.00 /83.50
bg	95/96	97/99	-/-	100/100	91/92	98/97	90/92	78/76	68/68	89.63/ 90.00
bf	83/91	93/95	96/99	-/-	93/97	97/99	95/95	85/84	73/71	89.38/ 91.37
ba	75/79	77/85	89/94	91/96	-/-	90/95	87/94	81/82	67/70	82.13/ 86.38
be	86/83	91/88	96/96	98/99	90/99	-/-	99/100	97	84	92.50/ 93.25
bd	79/78	84/83	90/90	91/95	90/89	98/98	-/-	98	84/86	89.25/ 89.63
bc	75/70	73/67	77/73	82/79	80/80	92/94	97/97	-/-	95/96	83.88 /82.00
bb	71/70	66/60	67/62	67/67	64/65	81/82	82/84	95/95	-/-	74.13 /73.12

5 hand annotated fiducial locations using 5 scales and 8 orientations resulting in 200 local classifiers which they fuse using the technique given in [22]. The method involves modeling the conditional probability of the Gabor response g_i of classifier i for same and different identities i.e. $P(g_i|same)$ and $P(g_i|dif)$ respectively. Then, Bayes Rule is used to obtain posteriors $P(same|g_i)$ and $P(dif|g_i)$ and the probability of final classification is the sum of the posterior probabilities. The inclusion of Gabor features has improved the accuracy dramatically because they are more discriminative than intensity features. Moreover, using Gabor features at hand-annotated fiducial landmarks is providing manual correspondence to the learning method. Combining Gabor features with probabilistic fusion is interesting and worth trying within our framework. Surprisingly, for CMU PIE our simple PLS based approach even outperformed the Gabor feature based approach.

Table 5: comparison of ADMCLS⁴⁰ with other published works on feret with frontal gallery.

Method	Probe pose								
	bi	bh	bg	bf	be	bd	bc	bb	Avg
LDA [38]	18.0	55.0	78.0	95.0	90.0	78.0	48.0	24.0	60.8
LLR [13]	45.0	55.0	90.0	93.0	90.0	80.0	54.0	38.0	68.1
CCA [13]	65.0	81.0	93.0	94.0	93.0	89.0	80.0	65.0	82.5
Stack [39]	40.0	67.5	88.5	96.5	94.5	86.0	62.5	38.0	71.7
Yamada [22]	8.5	32.5	74.0	88.0	83.0	54.0	23.5	6.5	46.3
Ridge [38]	67.0	77.0	90.0	91.0	92.0	89.0	78.0	69.0	81.6
DMCLS ⁴⁰	75.0	77.0	89.0	91.0	90.0	87.0	81.0	67.0	82.1
ADMCLS⁴⁰	79.0	85.0	94.0	96.0	95.0	90.0	82.0	70.0	86.4
<i>3DMM</i> [5]	<i>90.7</i>	<i>95.4</i>	<i>96.4</i>	<i>97.4</i>	<i>99.5</i>	<i>96.9</i>	<i>95.4</i>	<i>94.8</i>	<i>95.8</i>
<i>Gabor</i> [38]	<i>87.0</i>	<i>96.0</i>	<i>99.0</i>	<i>98.0</i>	<i>96.0</i>	<i>96.0</i>	<i>91.0</i>	<i>78.0</i>	<i>92.6</i>

5.3. Multi PIE

MultiPIE is an extension of CMU PIE data set containing more subjects and more pose-variation. It has a total 337 subjects photographed in 4 different sessions, under 15 different poses, 20 illumination conditions and 4 different expressions. We only took neutral expression and frontal lighting images for our experiments. All the pre-processing steps are the same as in CMU PIE except that the cropped facial region is 40×40 pixels. We took subject ID 1 to 100 as training and 101 to 346 as testing, resulting in a total of 237 testing subjects. For MultiPIE we could not obtain MCLS using all the poses in the training set due to memory problem associated with large eigen-value problem. Hence, we adopt the ADMCLS approach to select a subset of training poses and report the accuracy in Table 6. The MultiPIE data is relatively new and not many results are reported for pose invariant face recognition on it. We show our results along with the results of other works in Fig.13. It should be noted that we are reporting the results of [38] with pixels intensities as feature. Interestingly, our 2D approach is better than the 3D GEM [34] approach. We also observe that our approach is comparable to the approach in [38] for small pose differences but the difference increases with the pose angle. This might be due to the fact they report their result under frontal gallery and non-frontal probe only, giving them the opportunity to better tune the parameter but we report the result under general pose variation and do not optimize our method for frontal gallery and non-frontal pose. Moreover, we have outperformed [38] on both CMU PIE and FERET by large margins.

6. Conclusion and Discussion

We have proposed a generic Discriminative Coupled Latent Subspace based method for pose invariant face recognition. The learned set of coupled subspaces projects the images of the same person under different poses to close locations in

Table 6: MultiPIE accuracy for all possible 210 gallery-probe pairs using ADMCLS²⁵ with 237 testing subjects. The duplet below the pose name indicates the horizontal, vertical angle i.e. 45,15 means 45° horizontal and 15° vertical angle.

Prb→ Gal↓	110 -90,0	120 -75,0	090 -60,0	081 -45,45	080 -45,0	130 -30,0	140 -15,0	051 0,0	050 15,0	041 30,0	190 45,0	191 45,45	200 60,0	010 75,0	240 90,0	Avg
110	-/-	76.4	65.8	34.6	48.5	37.6	33.3	27.4	21.9	31.6	31.2	24.9	35.9	49.4	43.9	37.5
120	78.5	-/-	81.9	48.5	68.8	57.8	54.9	43.9	42.2	44.7	44.7	27.4	59.1	65.0	50.2	51.2
090	67.1	81.9	-/-	59.5	80.2	72.2	51.9	46.0	46.8	54.0	55.3	32.1	64.1	60.8	43.0	54.3
081	38.0	49.8	57.8	-/-	78.5	82.3	73.8	55.7	48.9	52.3	57.0	63.7	49.8	40.1	28.7	51.8
080	55.3	70.9	78.9	76.8	-/-	97.9	93.2	85.7	84.8	82.7	84.0	54.0	72.6	59.9	40.1	69.1
130	39.7	58.6	72.6	84.4	97.0	-/-	96.2	93.7	92.8	90.7	86.9	60.8	68.4	54.9	33.8	68.7
140	30.4	52.7	57.0	73.8	90.7	97.5	-/-	98.7	95.4	92.8	89.0	60.8	64.1	45.6	24.1	64.8
051	27.0	42.2	48.5	58.6	84.8	96.6	99.2	-/-	99.2	96.2	89.0	65.0	57.4	47.7	27.8	62.6
050	25.7	40.9	47.7	54.0	85.2	95.4	97.5	98.7	-/-	98.7	94.9	74.7	75.1	59.5	35.9	65.6
041	26.6	50.2	51.9	52.3	81.0	93.7	95.8	94.9	98.7	-/-	96.6	88.6	80.6	72.6	43.9	68.5
190	27.6	50.2	51.9	53.2	78.9	86.1	89.9	87.8	94.5	97.5	-/-	85.7	90.3	70.0	53.6	67.8
191	22.8	30.8	30.8	65.0	49.8	65.8	60.8	62.4	70.0	87.3	83.1	-/-	77.2	63.3	39.2	53.9
200	36.3	59.1	65.8	52.3	72.2	67.9	63.7	58.6	72.2	84.4	87.3	81.0	97.0	75.1	64.9	64.9
010	44.7	63.7	61.6	43.0	64.6	53.2	47.7	54.0	63.7	77.6	75.5	65.4	95.4	-/-	94.9	60.3
240	43.5	52.3	43.0	26.6	41.8	31.6	28.3	22.4	34.6	45.6	51.1	38.8	79.7	93.2	-/-	42.2

the latent space, making recognition possible using simple 1-NN or discriminative learning. We have discussed the conditions for such projection directions to exist and perform accurately. We further exploit the property of CCA to couple more than two subspaces corresponding to different poses and show that judiciously using multiple poses to learn the coupled subspace performs better than using just two poses. That is because information from multiple views is more consistent and robust to noise than just two views. Multiple coupled subspaces also provide us with the opportunity to generate multiple samples of a person in the latent subspace which can be used with LDA to encode discriminative information. We have provided empirical evidence that at pose-invariant-face recognition suffers from pose errors even under controlled settings, leading to poor performance. We tackle the pose error problem by artificially simulating pose error scenarios via adjacent-pose-latent projection. The latent projections obtained by projecting the images of a person under different poses on the same and adjacent pose projectors are used with LDA to effectively avoid the drop in performance due to small pose errors. The proposed approach has achieved state-of-the-art results on CMU PIE and FERET when 4 fiducial points are used with simple intensity features and comparable results on MultiPIE.

We experiment with pose variation only and illumination is considered to be constant. However, owing to the independent block structure of the overall framework, it can be easily extended to handle lighting variations by using some illumination invariant representation such as: The Self Quotient Image [46], Oriented gradient [47] etc... Moreover, Gabor features extracted at specific fiducial locations can be used to improve the performance further as in [38, 14, 15]. The coupled subspaces are learned in generative manner and only after projection on these subspaces, label information is used with LDA. The method could be improved by learning a discriminative coupled subspace directly. Learning such a subspace and using it for pose and lighting invariant face recognition is one of our future endeavors.

References

- [1] P. Santemiz, L.J. Spreeuwens and N.J.R. Veldhuis, "Side-View Face Recognition," In Proc. 32nd WIC Symposium on Information Theory in the Benelux, 10-11 May 2011.
- [2] S Lucey and T. Chen, "A viewpoint invariant, sparsely registered, patch based, face verifier," Int. Journal of Computer Vision, Vol. 80, pp. 58-71, 2008.
- [3] X. Jhang and Y Gao, "Face recognition across pose:A review," Pattern Recognition vol. 42, pp. 2876-2896, 2009.
- [4] A. Wagner, J. Wright, A. Ganesh, Z. Zhou, and Y. Ma, "Towards a practical face recognition system: Robust registration and illumination by sparse representation," CVPR, IEEE, pp. 597604, 2009.
- [5] V. Blanz and T. Vetter, "Face recognition based on fitting a 3d morphable model," IEEE TPAMI, vol. 25, no. 9, pp. 1063-1074, 2003.
- [6] The Facial Recognition Technology (FERET) Database, http://www.itl.nist.gov/iad/humanid/feret/feret_master.html
- [7] D.L. Swets and J. Weng, "Using discriminant eigenfeatures for image retrieval," IEEE TPAMI, vol. 18, no. 8, pp. 831-836, 1996.
- [8] S. Shan, Y. Chang, W. Gao, B. Cao and P. Yang, "Curse of mis-alignment in face recognition: problem and a novel mis-alignment learning solution," IEEE conf. Automatic Face and Gesture Recognition, pp. 314-320, 2004.
- [9] A. Sharma, A. Dubey, P. Tripathi and V. Kumar, "Pose invariant virtual classifiers from single training image using novel hybrid-eigenfaces," Neurocomputing, vol. 73, no. 10, pp. 1868-1880, 2010.
- [10] P.N. Belhumeur, J. Hespanha and D.J. Kriegman, Eigenfaces vs.Fisherfaces: recognition using class specific linear projection, IEEE TPAMI, Vol. 19, pp. 711-720, 1997.
- [11] A. Sharma and D.W. Jacobs, "Bypassing Synthesis: PLS for Face Recognition with Pose, Low-Resolution and Sketch," Proc. IEEE Conf. CVPR, pp. 593-600, 2011.
- [12] X. Chai, S. Shan, X. Chen and W. Gao, "Locally Linear Regression for Pose Invariant Face Recognition," IEEE Tran. Image Processing, vol. 16, no. 7, pp. 1716-1725, 2007.
- [13] A. Li, S. Shan, X. Chen and W. Gao, "Maximizing Intra-individual Correlations for Face Recognition Across Pose Differences," Proc. IEEE Conf. CVPR, pp. 605-611, 2009.

- [14] S.J.D. Prince, J.H. Elder, J. Warrell and F.M. Felisberti, "Tied Factor Analysis for Face Recognition across Large Pose Differences," *IEEE Patt. Anal. Mach. Intell.*, vol. 30, no. 6, pp. 970-984, 2008.
- [15] S.J.D. Prince, P. Li, Y. Fu, U. Mohammed and J. Elder, "Probabilistic Models for Inference about Identity," *IEEE TPAMI*, 13 May. 2011. <http://doi.ieeecomputersociety.org/10.1109/TPAMI.2011.104>
- [16] P. Phillips, H. Wechsler, J. Huang, and P.J. Rauss, "The FERET Database and Evaluation Procedure for Face Recognition Algorithms," *Image and Vision Computing*, vol. 16, pp. 295-306, 1998.
- [17] J.B. Tenenbaum and W.T. Freeman, "Separating style and content with bilinear models," *Neural Comp.* vol. 12, no. 6, pp. 1247-1283, 2000.
- [18] D.R. Hardoon, S.R. Szedmak and J.R. Shawe-Taylor, "Canonical correlation analysis: An overview with application to learning methods," *Neural Computation*, vol. 16, pp. 2639-2664, 2004.
- [19] R. Rosipal and N. Krämer, "Overview and recent advances in partial least squares," In *Subspace, latent structure and feature selection techniques*, Lecture Notes in Computer Science, Springer, pp. 34-51, 2006.
- [20] Partial Least Square Tutorial, <http://www.statsoft.com/textbook/partial-least-squares/#SIMPLS>.
- [21] T. Sim, S. Baker, and M. Bsat, "The CMU Pose, Illumination, and Expression Database," *IEEE Trans. Patt. Anal. Machine Intelligence*, vol. 25, no. 12, pp. 1615-1618, 2003.
- [22] T. Kanade and A. Yamada, "Multi-Subregion Based Probabilistic Approach Toward Pose-Invariant Face Recognition," *Proc. IEEE Conf. CIRA*, pp. 954-959, 2003.
- [23] C. Dhanjal, S.R. Gunn and J.S. Taylor, "Efficient sparse kernel feature extraction based on partial least squares," *IEEE Patt. Anal. Mach. Intell.* vol. 31, no. 8, pp. 1947-1961, 2009.
- [24] J. Baeka and M. Kimb, "Face recognition using partial least squares components, *Pattern Recognition*," vol. 37, pp. 1303-1306, 2004.
- [25] V. Struc and N. Pavesic, "Gabor-based kernel partial-least-squares discrimination features for face recognition," *Informatica*, vol. 20, no. 1, 2009.
- [26] X. Li, J Ma and S. Lia, "Novel face recognition method based on a principal component analysis and kernel partial least square," *IEEE ROBIO 2007*, pp. 1773-1777.
- [27] W.R. Schwartz, H. Guo, L.S. Davis, "A Robust and Scalable Approach to Face Identification," *Proc. ECCV*, pp. 476-489, 2010.

- [28] M.Turk and A.Pentland, "Eigenfaces for recognition," *Journal Cognitive Neuroscience*, vol. 3, no. 1, pp. 71-86, 1991.
- [29] R. Gross, I. Matthews, J. Cohn, T. Kanade and S. Baker, "MultiPIE," *Image and Vision Computing*, Vol. 28, no. 5, pp. 807-813, 2010.
- [30] M.B. Blaschko and C.H. Lampert, "Correlational Spectral Clustering," *CVPR*, pp. 1-8, 2008.
- [31] C.D. Castillo and D.W. Jacobs, "Using Stereo Matching with General Epipolar Geometry for 2-D Face Recognition Across Pose," *IEEE TPAMI*, vol.31, no. 12, pp. 2298-2304, 2009.
- [32] C.D. Castillo and D.W. Jacobs, "Wide-Baseline Stereo for Face Recognition with Large Pose Variation," *Proc. IEEE CVPR*, pp. 537-544, 2011.
- [33] R. Gross, I. Matthews, S. Baker, "Appearance-based face recognition and light- fields," *IEEE TPAMI* vol.26, no.4, pp. 449-465, 2004.
- [34] U. Prabhu, J Heo and M. Savvides, "Unconstrained Pose Invariant Face Recognition using 3D Generic Elastic Models,"
- [35] T. Ojala, M. Pietikainen and T. Maenpaa, "Multiresolution gray-scale and rotation invariant texture classification with local binary patterns," *IEEE TPAMI*, vol. 24, no. 7, 2002.
- [36] D. Lowe, "Distinctive image features from scale-invariant keypoints," *International Journal of Computer Vision*, vol. 60, no. 2, 91-110, 2004.
- [37] L. Wiskott, J. Fellous, N. Kruger and C. Von der Malsburg, "Face recognition by elastic bunch graph matching," *IEEE TPAMI*, vol. 19, no. 7, 1997.
- [38] A. Li, S Shan and W Gao, "Coupled Bias-Variance Trade off for Cross-Pose Face Recognition," *IEEE Transaction Image Processing*, 2011.
- [39] A. B. Ashraf, S. Lucey and T. Chen, "Learning patch correspondences for improved viewpoint invariant face recognition," In *CVPR*, June 2008.
- [40] Q. Ying, X. Tang and J. Sun, "An Associate-Predict Model for Face Recognition," In *CVPR* 2010.
- [41] S. Baker and I. Matthews, "Lucas-kanade 20 years on: A unifying framework," *International Journal of Computer Vision*, vol. 56, no. 3, pp. 221-255, 2004.
- [42] C.M. Bishop, "Pattern Recognition and Machine Learning," First Edition, Springer, 2006.
- [43] D.L. Swets and J. Weng, "Using discriminant eigenfeatures for image retrieval," *IEEE TPAMI* vol. 18, no. 8, pp. 831-836, 1996.

- [44] X. Liu and T. Chen, "Pose-robust face recognition using geometry assisted probabilistic modeling," IEEE CVPR, vol. 1, pp. 502509, 2005.
- [45] Z. Cao, Q. Yin, J. Sun and X. Tang, "Face recognition with learning-based Descriptor," In Proc. IEEE CVPR, 2010.
- [46] H. Wang, S.Z. Li and Y. Wang, "Face Recognition under Varying Lighting Conditions Using Self Quotient Image," in Proc. IEEE Int. Conf. Automatic Face and Gesture Recognition, pp. 819, 2004.
- [47] H.F. Chen, P.N. Belhumeur and D.W. Jacobs, "In search of illumination invariance," in Proc. CVPR, pp. 254-261, 2000.